Ecological Modelling 477 (2023) 110277

Contents lists available at ScienceDirect

Ecological Modelling

journal homepage: www.elsevier.com/locate/ecolmodel

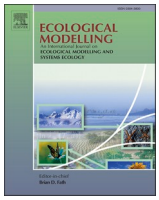

An aridity threshold model of fire sizes and annual area burned in extensively forested ecoregions of the western USA

Paul D. Henne *, Todd J. Hawbaker

U.S. Geological Survey, Geosciences and Environmental Change Science Center, Denver Federal Center, P.O. Box 25046, MS 980, Denver, CO 80225, United States

ARTICLE INFO

Keywords:
Climate change
Extreme events
Fire ecology
Global climate models
Rocky mountains
Water deficit

ABSTRACT

Wildfire occurrence varies among regions and through time due to the long-term impacts of climate on fuel structure and short-term impacts on fuel flammability. Identifying the climatic conditions that trigger extensive fire years at regional scales can enable development of area burned models that are both spatially and temporally robust, which is crucial for understanding the impacts of past and future climate change. We identified region-specific thresholds in fire-season aridity that distinguish years with limited, moderate, and extensive area burned for 11 extensively forested ecoregions in the western United States. We developed a new area burned model using these relationships and demonstrate its application in the Southern Rocky Mountains using climate projections from five global climate models (GCMs) that bracket the range of projected changes in aridity. We used the aridity thresholds to classify each simulation year as having limited, moderate, or extensive area burned and defined fire-size distributions from historical fire records for these categories. We simulated individual fires from a regression relating fire season aridity to the annual number of fires and drew fire sizes from the corresponding fire-size distributions. We project dramatic increases in area burned after 2020 under most GCMs and after 2060 with all GCMs as the frequency of extensive fire years increases. Our adaptable model can readily incorporate new observations (e.g., extreme fire years) to directly address the non-stationarity of fire-climate relationships as climatic conditions diverge from past observations. Our aridity threshold fire model provides a simple yet spatially robust approach to project regional changes in area burned with broad applicability to ecosystem and vegetation simulation models.

1. Introduction

Fire is the dominant disturbance in many forested regions of the world, and many forest species possess adaptations to survive, or regenerate after, fire (Bond et al., 2005; Bowman et al., 2009). However, annual area burned increased dramatically in recent years in concert with rising regional temperatures, bringing record-breaking fire seasons to western North America, Siberia, and Australia in 2019/2020 alone, and prompting concern that observed and projected climatic changes will further increase fire activity (Collins et al., 2021; Higuera and Abatzoglou, 2021; Ponomarev et al., 2021). Such changes have well-documented societal and ecological consequences; extensive wildfires produce hazardous air, increase spending on fire management and emergency services, drive shifts in species abundances, and even trigger the replacement of forests with open and shrub-dominated ecosystems (Bowman et al., 2017; Davis et al., 2019; Turner, 2010). Therefore, anticipating changes in fire frequency, fire size, and annual area burned is critical to understanding the societal and ecological risks posed by wildfire.

Annual area burned is a key statistic used to track changes in wildfire activity through time and can be quantitatively linked to the climatic, ecological, and cultural factors that constrain fire regimes. Area burned increased in many ecosystems, not only during recent drought events, but also during warm, dry intervals of the past (Calder et al., 2015; Higuera et al., 2021; Marlon et al., 2012; Westerling et al., 2006), which demonstrates an enduring link between climate and fire activity. Climate has both long and short-term impacts on fire activity. On annual and longer timescales, climate constrains vegetation dynamics and therefore fuel availability (including fine fuels) and fuel connectivity. In the short term, climate controls fuel moisture, which decreases under dry conditions, increasing flammability, and fire spread. Changes in fuel moisture can be tracked using aridity indices, including water-balance or fire-danger metrics that synthesize the interactions among temperature, precipitation, and soil water (Littell et al., 2016). Although fuel

* Corresponding author.
E-mail address: phenne@usgs.gov (P.D. Henne).

https://doi.org/10.1016/j.ecolmodel.2023.110277
Received 7 October 2021; Received in revised form 23 November 2022; Accepted 4 January 2023
Available online 11 January 2023

moisture is an important driver of annual variability in area burned, the specific climatic conditions that engender extensive fire years vary among ecosystems and vegetation types and are affected by disturbance and management histories (Littell et al., 2009; Westerling et al., 2003). Nonetheless, recent analyses demonstrated significant correlations between aridity indices and area burned at monthly to annual scales (Abatzoglou and Kolden, 2013; Williams et al., 2015). Furthermore, exponential increases in area burned have been reported in many forested regions when fire-season aridity exceeds a threshold (Henne et al., 2021; Pausas and Paula, 2012; Young et al., 2017).

Fire models provide a means to understand the drivers of past variation in area burned and anticipate future change. Models operate at varying scales of area and complexity, with associated tradeoffs in realism and computational intensity. Statistical and machine learning models relate one or more predictor variables to fire regime components at pixel, regional, and subcontinental scales (Jain et al., 2020; Xi et al., 2019). Although input variables differ among models, those relying on aridity indices as a proxy for fuel moisture often show similar performance as models that rely on multiple predictors (Higuera et al., 2015; Williams et al., 2015). Combined statistical models can simulate both ignition numbers and fire sizes (Westerling et al., 2011) that can be applied to, or integrated with, landscape vegetation models to investigate wildfire impacts on vegetation dynamics. Although landscape models are often calibrated with historical fire return intervals or observed fire-size distributions (He and Mladenoff, 1999), ignition probabilities and fire-size distributions may also be related to climatic parameters to project climate-change impacts (Henne et al., 2021; Liang et al., 2017). More data-intensive approaches incorporate landscape- and fuel-specific data. For example, models that predict fire spread based on fuel characteristics and topography can use spatially explicit information to understand fire risks across landscapes (Finney et al., 2011; Liu et al., 2015; Sleeter et al., 2015). While such models can apply empirical fire-behavior data, they can require extensive calibration, demand detailed information about fuel composition and condition over time, and may have unrealistic assumptions about fuel behavior when applied to novel settings. At regional to global scales, dynamic global vegetation models (DGVMs) use observed relationships among fuel moisture, fire season length, and burned area, or processed-based estimations of fire ignition and spread (e.g., Thonicke et al., 2001; Li et al., 2012). However, large differences exist among models in the representation of processes that constrain burned area, and additional model complexity does not necessarily improve model performance, which can vary regionally (Hantsen et al. 2016). Despite the extensive efforts to simulate fires and area burned, there remains a need for computationally efficient fire models that can easily integrate with simulation models, incorporate recent patterns of fire occurrence, and allow for rapid assessment of future potential changes in fire occurrence.

Here, we investigate relationships among fire season aridity, the annual number of fires, and annual area burned in 11 extensively forested ecoregions of the western United States (Fig. 1). We focus on extensively forested ecoregions because of their known sensitivity to annual variations in fire-season aridity relative to non-forested ecoregions (Littell et al., 2018). For each ecoregion, we identify significant relationships between fire-season aridity and the annual number of fires, and thresholds in fire-season aridity that separate years with significant differences in area burned. We use these ecoregion-specific data to develop a model that uses aridity thresholds to project climate-driven changes in the number of fires, generates fire sizes, and calculates annual area burned. In a final step, we apply the model to simulate climate-driven changes in annual area burned in the Southern Rocky Mountains ecoregion using climate projections for 2021 – 2100.

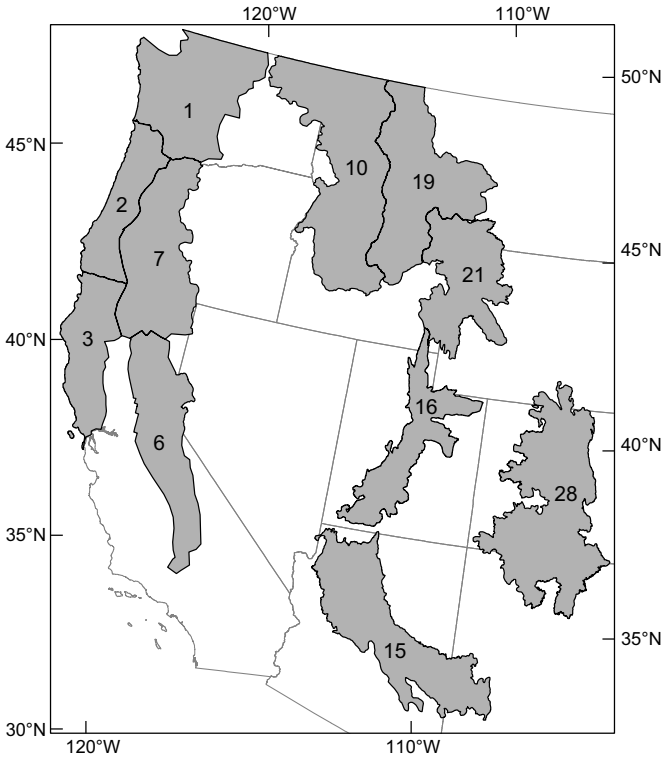

Fig. 1. The western United States, with extensively forested ecoregions (Homer et al., 2015) shown in gray. See Table 1 for ecoregion names. State boundaries (gray lines) are shown for reference.

2. Methods

2.1. Quantifying annual area burned and fire-season climatic water deficit (FSCWD) for 1980 – 2020

We investigated relationships among seasonal drought, the annual number of large fires, and annual area burned in 11, extensively forested ecoregions in the western United States (Fig. 1). We used ecoregions defined by National Land Cover Database (NLCD) mapping zones as our unit of analysis (Homer et al., 2015). Vegetation ranges from alpine tundra to subalpine and montane forests, open woodlands, sagebrush steppe, and semiarid grasslands in these mountainous ecoregions. We compiled annual area burned records for each ecoregion from 1980 – 2020 (see Supporting Information).

We calculated monthly climatic water deficit (CWD; Stephenson, 1998) as a proxy for fuel aridity at the ecoregion scale. Defined as the difference between potential evapotranspiration (PET) and actual evapotranspiration (AET), CWD quantifies evaporative demand unmet by soil water. We used reference evapotranspiration (ET_o, ASCE Penman-Montieth; Abatzoglou, 2013) to represent PET and estimated monthly AET with the soil water balance model used by the LANDIS-II forest landscape model, NECN extension (Scheller et al., 2021; see Supporting Information). We summarized monthly CWD and area burned at the ecoregion level. We used the same fire season for all ecoregions, defined as the months that captured >95% of area burned for the entire study region, then summed monthly CWD values to assign an annual fire-season CWD (FSCWD) for 1980 – 2020 to each ecoregion. This resulted in annual values for FSCWD and area burned for each ecoregion.

2.2. Relationships between fire-season aridity, the annual number of large fires, and area burned

Whereas most fires in western North America are small (i.e., < 1 ha),

large fires account for most area burned (Short, 2021). We analyzed only large fires, defined as those fires that cumulatively contributed > 99% of total burned area in each ecoregion from 1980 – 2020 by identifying separate large-fire-size thresholds for each ecoregion. For each ecoregion, we fit a linear regression between the FSCWD and the annual number of large fires using all 41 years of the calibration period. We also fit 41 separate regressions using 40 years of data as part of a leave-one-year-out analysis.

Annual area burned does not increase linearly with aridity in extensively forested ecoregions of western North America. Instead, area burned tends to be extensive when fuel aridity exceeds quantifiable aridity thresholds (AT), and limited or moderate in fire seasons that do not exceed these thresholds. We identified ATs for each ecoregion by relating annual area burned to FSCWD using conditional inference trees (Hothorn et al., 2006) to separate years into either two or three area burned categories: limited, moderate, and extensive, or moderate and extensive (see Supplemental Information). For each ecoregion, we identified ATs with all 41 years of the calibration period, and with 40 years of data by leaving out each year once as part of a leave-one-year-out analysis.

2.3. Applying aridity thresholds to simulate climate change impacts on area burned

We evaluated model performance by simulating annual area burned in each ecoregion from 1980 to 2020 using historical climate. We first used the linear regressions to predict the annual number of large fires. To represent variability, we randomly selected the number of fires from a normal distribution defined by the regression's predicted value and standard error. To determine the size of each fire, we fit separate fire-size distributions to the groups of years defined with the ATs as being limited, moderate, or extensive fire years. We fit both lognormal and Pareto distribution functions, both of which produce long-tailed distributions suitable for representing our data where a small number of very large fires account for most area burned (Holmes et al., 2008) with the fitdistrplus package in R (Delignette-Muller and Dutang, 2015; R Core Team, 2022). We then drew random fire sizes from the limited, moderate, or extensive fire-size distributions depending on the value of the annual FSCWD relative to the lower and upper ATs and summed the area of all simulated fires for each year.

For each ecoregion, we generated 1000 41-year simulations from the full and leave-one-year-out datasets. We assessed model performance by calculating three metrics that compare observed to simulated area burned: root mean square error standardized by the standard deviation of annual area burned (RMSE / SD), mean error, and Pearson's correlation. RMSE measures accuracy and dividing by the standard deviation of observed annual area burned allows comparison among ecoregions; smaller values indicate greater model skill (Littell et al., 2009). We used mean error as a measure of bias, indicating simulations that over- or underestimate area burned relative to observations. The coefficient of determination (r^2) measures how well year-to-year variability in the predictions follow observations for the calibration period. We tested for temporal autocorrelation in the residuals of the modeled number of large fires and annual area burned with the acf function in R and plotted the distributions of residuals through time for all ecoregions and models to examine shifting biases in predictions.

To demonstrate how our modeling approach can be used to make projections, we simulated area burned under changing future climate for the Southern Rocky Mountains using the area burned model fit with all 41 years from the calibration period. We obtained temperature, precipitation, and reference evapotranspiration (ET_o) data from the period 1980 – 2100 for 13 global climate models (GCMs) under the RCP 8.5 emissions scenario that were downscaled to a 4 km grid using multivariate adapted construction analogues (MACA; Abatzoglou and Brown, 2012). We calculated GCM FSCWD as described above then ranked the 13 GCMs by FSCWD from 2020 – 2100 and selected 5 GCMs that represented the full range of projected aridity (i.e., the minimum, 1st quartile, median, 3rd quartile, and maximum FSCWD; Henne and Hawbaker, 2023).

3. Results

We set a fire season for our analyses of May-October, during which most fires (96%), and area burned (97%) were recorded in the 11 ecoregions. Within this fire season, the threshold for large fires that contributed >99% of area burned varied among ecoregions from 10 ha in the Utah High Plateaus to 80 ha in the Middle Rocky Mountains and Oregon Coastal Range (Table 1).

We found significant ($p < 0.01$), positive linear relationships between FSCWD and the number of large fires in all ecoregions. However, the strength of the correlations varied (Table 1). Ecoregions with a strong positive correlation (e.g., Middle Rocky Mountains, $r^2 = 0.69$) had large interannual variation in the number of large fires (Figs. 2a and S1), indicating a greater importance of fire-season climate as a determinant for the number of large fires. In ecoregions with a lower correlation, multiple large fires occurred in most years (e.g., Sierra Nevada Range, $r^2 = 0.18$).

We identified ATs that distinguish years with significant differences in annual area burned for all ecoregions (Table 1, Figs. 2b and S2). Two ecoregions, the Oregon, and California Coastal, ranges have one significant ($p < 0.05$) AT. We identified two significant ATs in the remaining ecoregions; a lower threshold (AT1) distinguishes years with limited and moderate area burned, and an upper threshold (AT2) separates years with moderate and extensive area burned (Table 1; Figure S2). For example, in the Southern Rocky Mountains, 30 years had limited (mean = 7979 ha), 7 years had moderate (mean = 32,652 ha), and 4 years had extensive (mean = 169,993 ha), area burned. All three divisions had a large number of fires to fit fire-size distributions. There were 634 fires in the limited area burned years, 255 fires in the moderate area burned years, and 251 fires in the extensive area burned years. Mean fire sizes in limited, moderate, and extensive fire years varied among ecoregions. In the Sierra Nevada Range and Mogollon Rim, where very large fires

Table 1
Extensively forested ecoregions in the western United States (Homer et al., 2015). Numbers in parentheses correspond to labels in Fig. 1. Fires larger than the large fire threshold comprise >99% of burned area in each ecoregion. Fires smaller than this threshold were omitted from the analyses. The coefficient of determination (r^2) values are for linear regressions relating fire-season climatic water deficit (FSCWD) to the annual number of large fires. All regressions are highly significant ($p < 0.01$). Aridity thresholds (AT1 and AT2) distinguish years with significantly different ($p < 0.05$) area burned. Years when FSCWD < AT1 tend to have limited area burned, years when AT1 > FSCWD < AT2 tend to have moderate area burned, and years when FSCWD > AT2 tend to have extensive area burned. AT values are FSCWD, standardized by subtracting the mean and dividing by the standard deviation of observed FSCWD from 1980 – 2009.

Ecoregion	Large fire threshold (ha)	Coefficient of determination (r^2)	AT1	AT2
Northern Cascades (1)	16	0.28	0.84	NA
Oregon Coastal Range (2)	16	0.26	1.33	NA
Northern California Coastal Range (3)	80	0.35	0.88	1.48
Sierra Nevada Range (6)	12	0.18	−0.03	1.17
Cascades Range (7)	16	0.24	0.28	0.99
Northwestern Rocky Mountains (10)	28	0.59	−0.31	0.36
Mogollon Rim (15)	14	0.20	−0.18	0.86
Utah High Plateaus (16)	10	0.37	−0.14	1.21
Northern Rocky Mountains (19)	25	0.39	−0.52	0.61
Middle Rocky Mountains (21)	80	0.69	0.47	1.25
Southern Rocky Mountains (28)	12	0.56	0.68	1.29

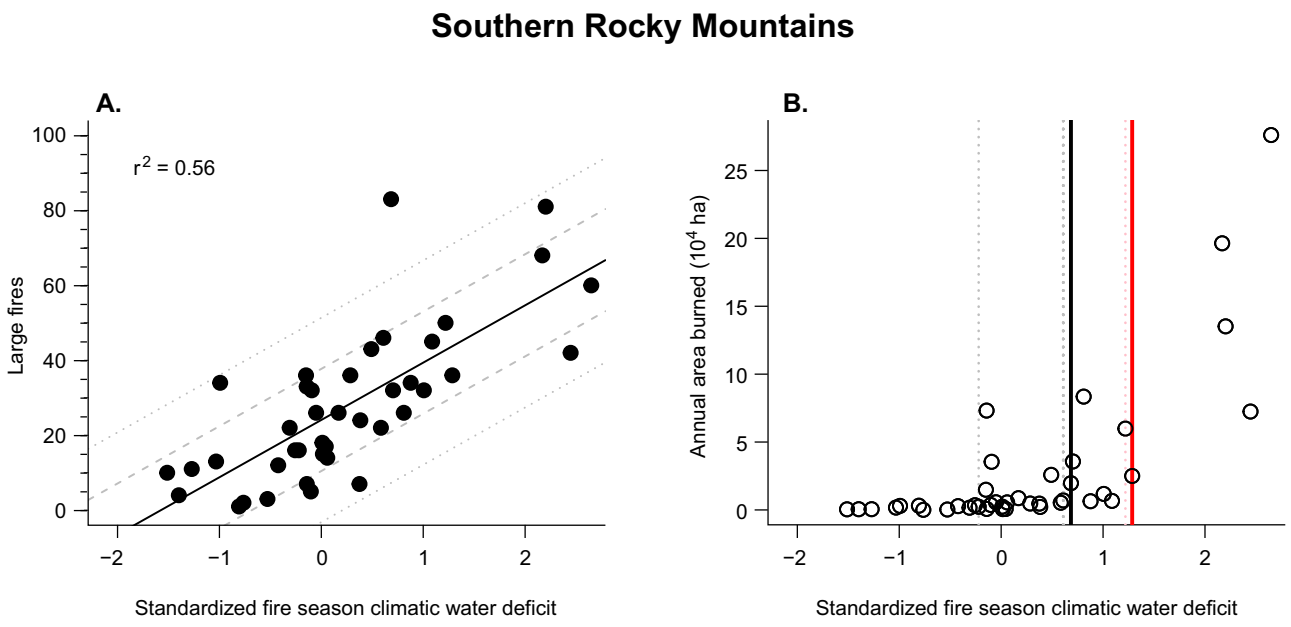

Fig. 2. A. Regression between the standardized fire-season climatic water deficit (FSCWD) and the number of fires larger than 12 ha in the Southern Rocky Mountains. The dashed gray lines show one standard error of the regression, and the dotted lines two. B. Aridity thresholds that distinguish groups of years with significant differences in area burned. Each circle denotes the FSCWD and area burned in a single year. The black line is the lower aridity threshold (AT1) that separates years with limited and moderate area burned. The red line is the upper aridity threshold (AT2) that separates years with moderate and extensive area burned. Gray dashed lines denote alternative AT1s identified with the leave-one-year-out analysis. Red dashed line denotes an alternative AT2.

occurred in even wetter-than-average years, mean area burned was > 22,000 ha during limited fire years. In contrast, in the Rocky Mountain ecoregions (i.e., Northwestern, Northern, Middle, and Southern Rocky Mountains), wet years dampened the number and size of fires, and limited fire years all averaged < 8000 ha (range of 502 – 7979 ha).

The leave-one-year-out analysis identified at least one alternate AT in all ecoregions. In most ecoregions, these alternate splits did not cause a major change in the number of years classified as limited, moderate, or extensive, indicating most individual years had no impact on the position of ATs (Figs. 2b, S2). However, in four ecoregions where area burned in a single year greatly exceeded area burned in all other years (i.e., the Northern California Coastal, Cascades, and Sierra Nevada ranges in 2020, and the Middle Rocky Mountains in 1988), removing the extreme fire year strongly affected the ATs. The Southern Rocky Mountains ecoregion provides an important contrast. There, 2020 had both the highest observed FSCWD and area burned. However, extreme fire years in 2002 and 2018 with a similarly high FSCWD (Fig. 2), meant that omitting 2020 did not shift the ATs.

3.1. Burned area simulations for 1980 – 2020

Observed fire-size distributions for limited, moderate, and extensive fire years were not significantly different ($p > 0.05$, Cramer-von Mises test) from the fitted lognormal and Pareto distributions in any ecoregion when calculated with all years. Because we used a random sample of observed fire sizes for the Cramer-von Mises tests, statistical distributions estimated for some years in the leave-one-year-out analysis were significantly different from the subset of observed fire sizes. However, on average, observed fire size distributions for limited, moderate, and extensive fire years were also not significantly different from the lognormal and Pareto distributions for the leave-one-year-out analysis for all ecoregions.

Simulated area burned tracked observed interannual variation in area burned for all ecoregions during the calibration period (Figs. 3 and S3; Henne and Hawbaker, 2023). Residuals for the mean simulated number of fires showed no significant autocorrelation in all ecoregions for most of the 1000 simulations for models calibrated with the full data set and models for the leave one-year-out analysis (Figure S4). Likewise, residuals of area burned simulated with lognormal and Pareto distributions were not autocorrelated for most replicates in all ecoregions with models trained with all years or the leave one-year-out analysis (Figure S5). Correlations between the mean simulated and observed annual area burned were significant in all ecoregions when models were trained using all years (p-value < 0.05) and r^2 ranged between 0.48 and 0.74 (Table S1). The type of fire-size distribution (lognormal or Pareto) had little influence on r^2 values. The largest difference was in the Utah High Plateaus (0.07 difference). However, individual years had a large influence on the correlation. Correlations were not significant in the leave-one-year-out analysis for the Sierra Nevada Range and Cascades Mountain Range. Whereas correlations remained significant for all other ecoregions, r^2 was consistently lower (i.e., 0.09 – 0.22 decrease).

Simulations with Pareto fire-size distributions better captured the observed range in area burned than simulations with lognormal distributions (Table S1). With lognormal distributions, observed area burned fell within the simulation range between 37 and 41 years in the different ecoregions (Figs. 3 and S3; Table S1). Most years with observed area burned outside the simulation range were underestimates of area burned for extensive fire years (e.g., 2020 in the Sierra Nevada Range). Overestimates occurred in one year in the Northern Cascades Range and two years in the Middle Rocky Mountains (Figure S3) because we assumed a minimum of one large fire in every year. This assumption is broadly consistent with fire records; no years lacked a recorded fire, and years without a large fire occurred in only the Northern Cascades (two years), Northern Rocky Mountains (one year), and Middle Rocky Mountains (three years). With Pareto fire-size distributions, observed area burned was less than the simulated maximum in all ecoregions and all years for models trained with the full dataset, but fell outside the simulation range with Pareto distributions in 2017 for the Oregon Coastal Range, and 2020 for the Sierra Nevada Range in the leave-one-year-out analysis.

Negative mean error values for all ecoregions indicate that fire simulations drawn from lognormal distributions generally underestimated total area burned; mean error ranged from -66% to −15% for models trained with all years, and from −66% to −14% for the leave-one-year-out models (Table S1). Drawing fire sizes from Pareto

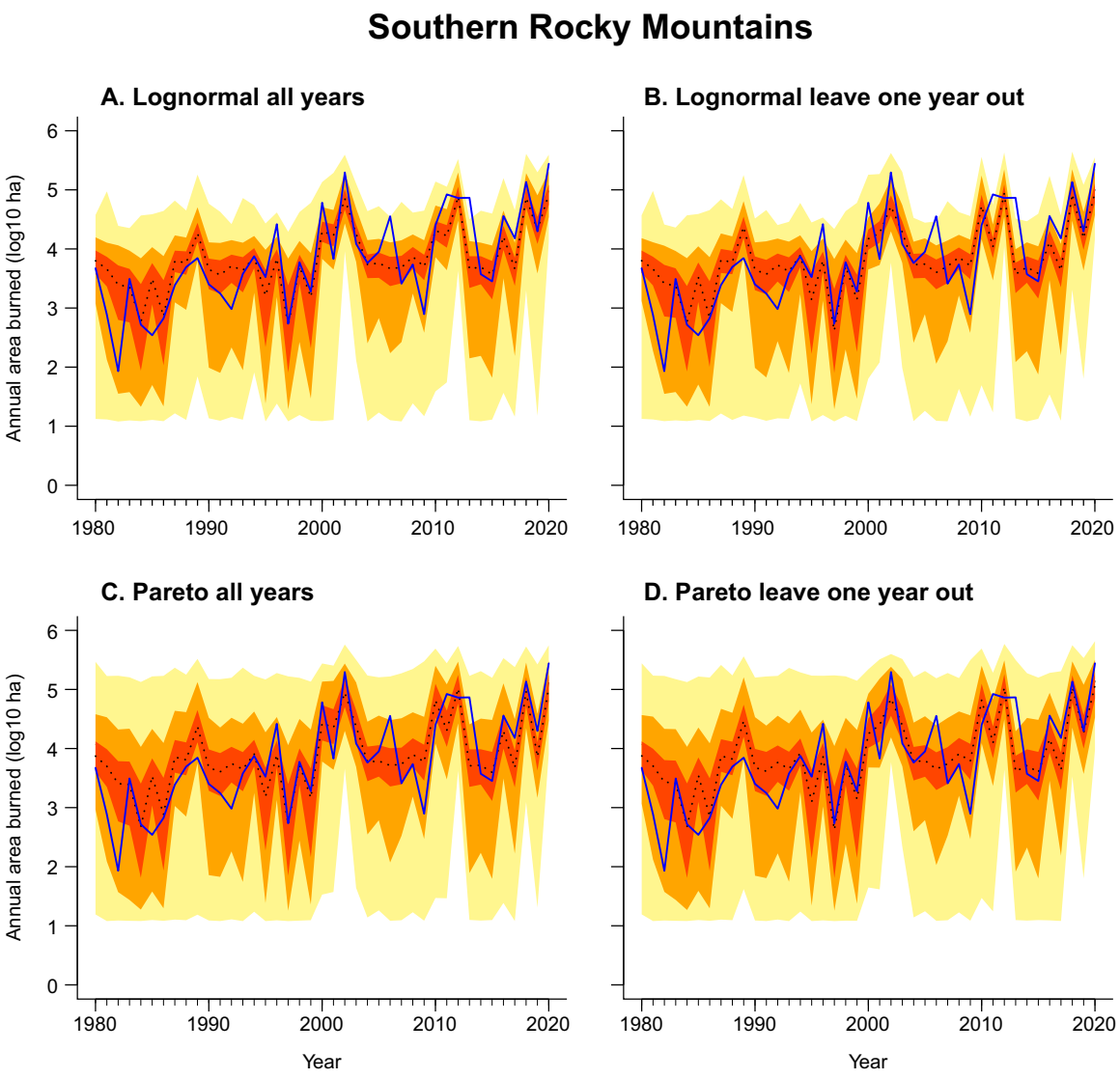

Fig. 3. Historical area burned simulations for the Southern Rocky Mountains. Blue lines show observed annual area burned. Dotted lines show the median of 1000 simulations. Red area shows the interquartile range, orange area the 5th to 90th percentile of simulated area burned, and yellow area the full simulation range. A. Fire sizes were drawn from lognormal distributions fit to all years (1980 – 2020). B. Fire sizes were drawn from lognormal distributions with the simulation year left out. C. Same as A. except using Pareto distributions. D. Same as B. except using Pareto distributions.

distributions, which include a higher probability of very large events, resulted in more simulated area burned. With Pareto distributions, mean error ranged from −44% to +47% when all years were considered, and −41% to +50% with the leave-one-year-out analysis. In most ecoregions, mean error was generally closer to zero with Pareto distributions. Time series of residuals show that model errors were not significantly different between models calibrated with all years and the leave-one-year-out analysis (Figures S6, S7). However, residuals were generally larger after 2000 when conditions generally became drier in the western US and observed area burned increased (Williams et al., 2020; McCabe and Wolock 2021).

Simulations with fire sizes drawn from Pareto distributions had higher RMSE/SD than those drawn from lognormal distributions, indicating lesser skill and wider dispersion of the simulation results (Table S1). Model skill was highest in the Southern Rocky Mountains with lognormal distributions (RMSE/SD = 0.75). Models using Pareto distributions showed moderate skill in the Southern Rocky Mountains (RMSE/SD = 0.85), and a small sensitivity to individual years (RMSE/SD = 0.89 for the leave-one-year-out analysis).

3.2. *Area burned projections for the Southern Rocky Mountains*

We selected five GCMs that span the range in FSCWD projected by the CMIP5 models for the period 2021 – 2099 (Henne and Hawbaker, 2023) and used annual FSCWD from these GCMs to simulate annual area burned. Observed FSCWD was on average higher (i.e., drier) than GCM FSCWD from 1981 – 2020, especially after 2000. Most years were classified as limited fire years in the historical (28 years) and GCM data (31 – 35 years). However, four years, 2002, 2012, 2018, and 2020, had drier fire seasons than all but one year in the five GCMs. The historical data also had more moderate fire years (six) than the GCMs, which ranged from two to five years. The GCM with the lowest FSCWD (CNRM-CM5) had one extensive fire year during the historical period, HadGEM2 with the highest FSCWD had five, and the remaining models three. Relatively low GCM FSCWD during the historical period (Figs. 4 and 5) may mean that the GCMs also underestimate FSCWD in the coming decades.

Separation among the GCMs and historical climate is evident after 2020 (Figs. 4, 5). From 2021 – 2060, the relatively moist CNRM-CM5 does not project drier fire seasons than the historical record. In

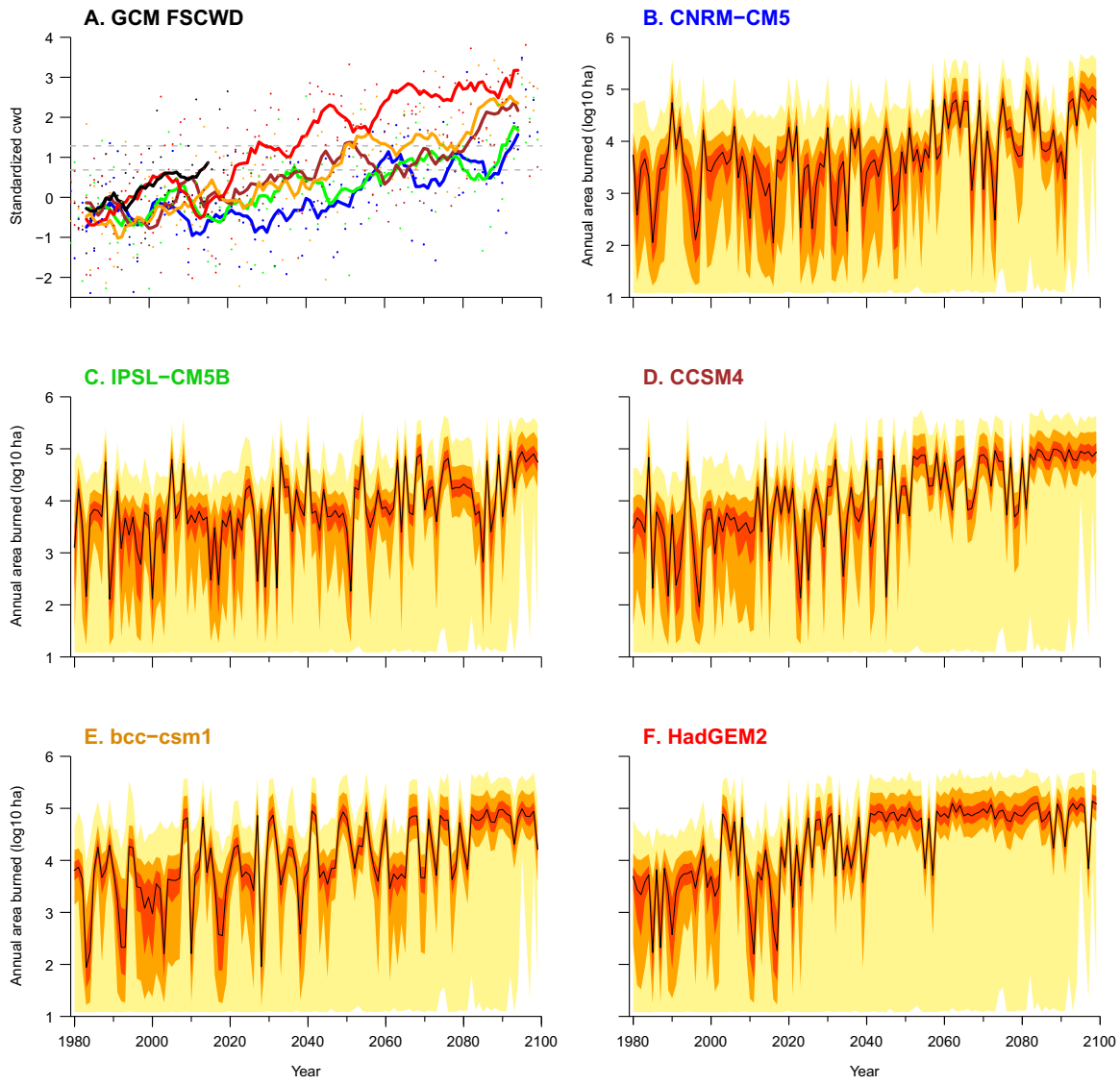

Fig. 4. A. Area-weighted annual fire-season climatic water deficit (FSCWD) for the Southern Rocky Mountains calculated for five downscaled global climate models (GCMs; colored lines) and observed climate (black line) for 1980 – 2020. Points show individual years, lines show a 10-year moving average. Dashed gray lines show the lower and upper aridity thresholds (AT1 and AT2). When the bold colored lines cross the dashed gray lines the average year is a moderate (i.e., > AT1) or extensive (i.e., > AT2) fire year. B – F. Same as Fig. 3A, except climate data were drawn from GCMs.

contrast, IPSL-CM5B, CCSM4, and bcc-csm1 which rank as the 1st quartile, median, and 3rd quartile of FSCWD all have 10 moderate fire seasons, but 3, 10, and 11 extensive years. HadGEM2 has six moderate and 25 extensive fire years in this same interval. During the final 40 years, from 2060 – 2099, most years are either moderate or extensive fire years for all GCMs. The two wettest GCMs (CNRM-CM5, IPSL-CM5B) maintained 14 limited fire years, and nine and 11 moderate fire years respectively. Most years are extensive fire years in the drier GCMs. CCSM4 has 25, bcc-csm1 30, and HadGEM2 37, extensive fire years. The frequency of extensive fire years may provide an important marker for changing fire-climate relationships. For the Southern Rocky Mountains, the timing of such a shift varies among GCMs. Under the extreme HadGEM2, average FSCWD exceeds the upper AT after 2038 (i.e., 10-year moving average FSCWD > AT2; Figs. 4a and 5a). The average FSCWD fluctuates near AT2 after 2050 with bcc-csm1 and remains above AT2 after the 2080s. Average FSCWD also remains above AT2 during the 2080s but does not exceed AT2 until the 2090s with the wetter CNRM-CM5 and IPSL-CM5B GCMs.

We summarized simulated area burned for the three 40-year periods with the median, range, and interquartile range to help visualize and compare long-term trends relative to the calibration period (Fig. 6). Observed area burned in the Southern Rocky Mountains from 1981 – 2020 exceeded the range of area burned simulated with observed climate and lognormal distributions. However, one year (i.e., 2020) had a major impact on this offset. In contrast, observed area burned fell within the interquartile range of simulations using Pareto distributions. Median simulated area burned was lower than observations for the historical period with all GCMs with lognormal (−49% – −76%) and Pareto (−23 – −60%) distributions, which was not surprising given that both the mean FSCWD and frequencies of moderate and extreme fire years are lower in the GCMs.

Simulated area burned increased in all GCMs during the period 2021 – 2060 (Fig. 6). Median area burned simulated with lognormal distributions remained below observed area burned from 1981 – 2020 for the two wettest scenarios, CNRM-CM5 (−65%) and IPSL-CM5B (−47%), was slightly higher for CCSM4 (+2%) and bcc-csm1(+3%), and about double (+101%) for HadGEM2, the driest GCM. For HadGEM2, the frequency of extreme fire years increased markedly after 2040 (Fig. 4). With Pareto distributions, the median simulated area burned for CNRM-CM5 and IPSL-SM5B from 2021 – 2060 was lower than observed from

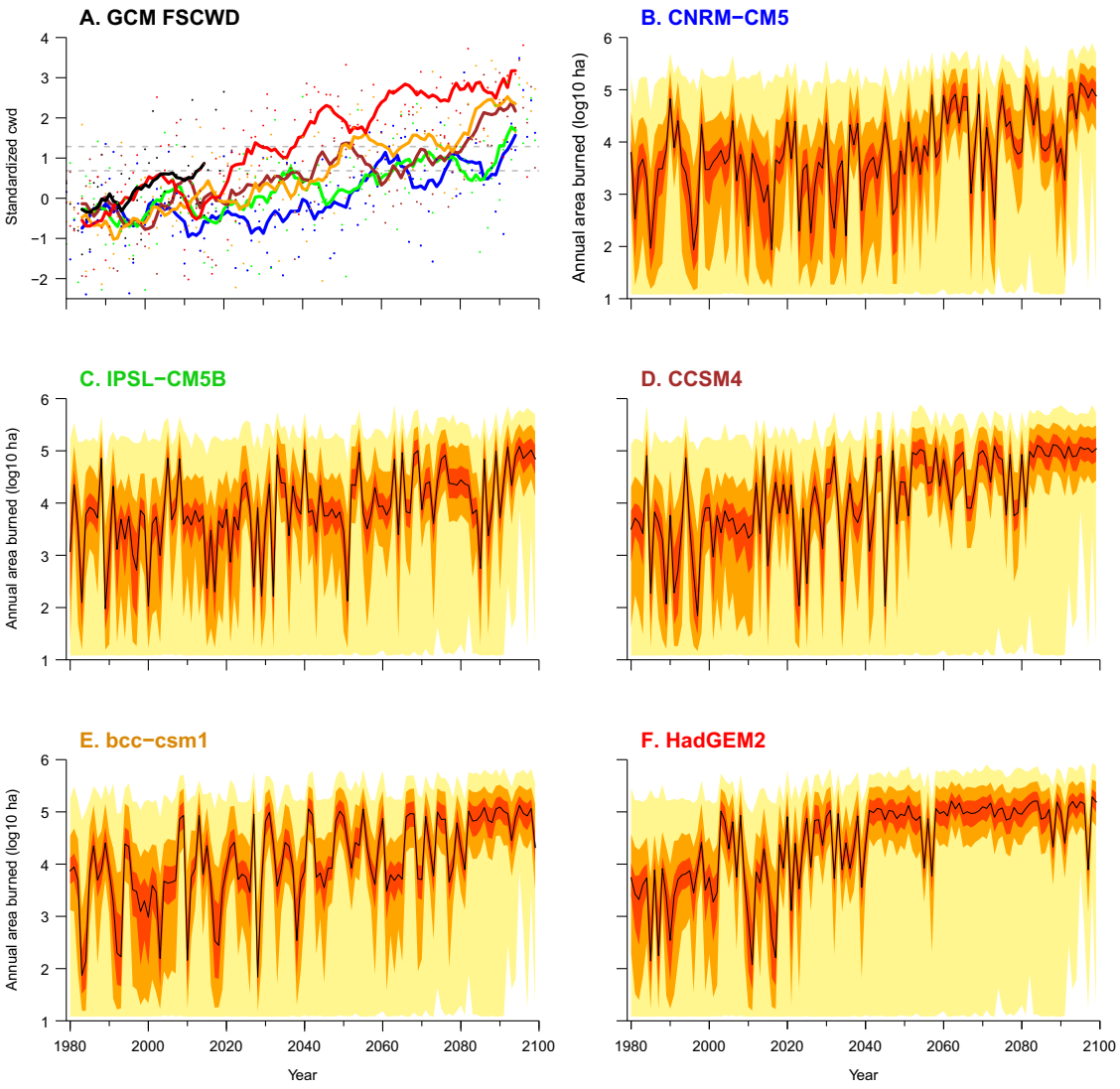

Fig. 5. Same as Fig. 4, except using Pareto distributions.

1981 – 2020 by −44% and −18%, but much higher with CCSM4 (+47), bcc-csm1 (+49%), and HadGEM2 (+174%). During the final 40 years of simulations, the increase in median simulated area burned relative to observed area burned in 1981 – 2020 ranged from +33 – +246% with lognormal distributions and +94 – +360% with Pareto distributions (Fig. 6).

4. Discussion

4.1. Aridity thresholds for limited, moderate, and extensive fire years

Fire-season climatic water deficit (FSCWD) effectively distinguishes years with limited, moderate, and extensive area burned in extensively forested ecoregions with variable land cover and climate. Water deficit metrics like FSCWD are robust predictors of annual area burned in forested regions because they integrate multiple factors that constrain fuel moisture (e.g., temperature, precipitation, insolation, soils). Although our burned area model relies on a single water deficit metric, we achieve similar predictive skill at the ecoregion scale as more complex models that integrate multiple variables (Littell et al., 2018, 2009). FSCWD also increases with fire-season length, a critical driver of recent increases in area burned (Westerling et al., 2006), because it sums monthly water deficits over a period that exceeds the typical fire season through much of our study area.

Aridity thresholds link area burned to fire-season water balance at the regional scale. However, flammability also varies within regions at finer scales. Warm, dry topographic settings (e.g., lower elevations, south-facing slopes) may experience flammable conditions during a typical year while adjacent north-facing slopes and upper elevations remain relatively moist (Dillon et al., 2011). Topographic position similarly affects productivity and therefore fuel loads (Kane et al., 2015; Rollins et al., 2002). Intraregional variation in fuel moisture and availability may explain the occurrence of two aridity thresholds in the ecoregions considered here, which include complex, mountainous terrain. In ecoregions with two ATs, flammable conditions are very unlikely at both local and regional scales during years with limited burning (i.e. FSCWD < AT1). For example, in the Southern Rocky Mountains, mean area burned is 7979 ha when FSCWD < AT1, probably because moist conditions limited fire spread through much of the ecoregion. In contrast, during years with moderate area burned (i.e., AT1 > FSCWD < AT2), mean area burned is 32,652 ha, and it is likely that the driest landscapes (e.g., submontane forests and grasslands at lower elevations or southerly aspects) become flammable. Years with extensive area burned (mean area burned = 169,993 ha) occur when regional climate overwhelms local heterogeneity in fuel moisture and fires readily spread in even typically moist settings (e.g., subalpine forests at high elevations and on northerly aspects). Extensive burning tends to coincide with high severity fires in forests of the western United

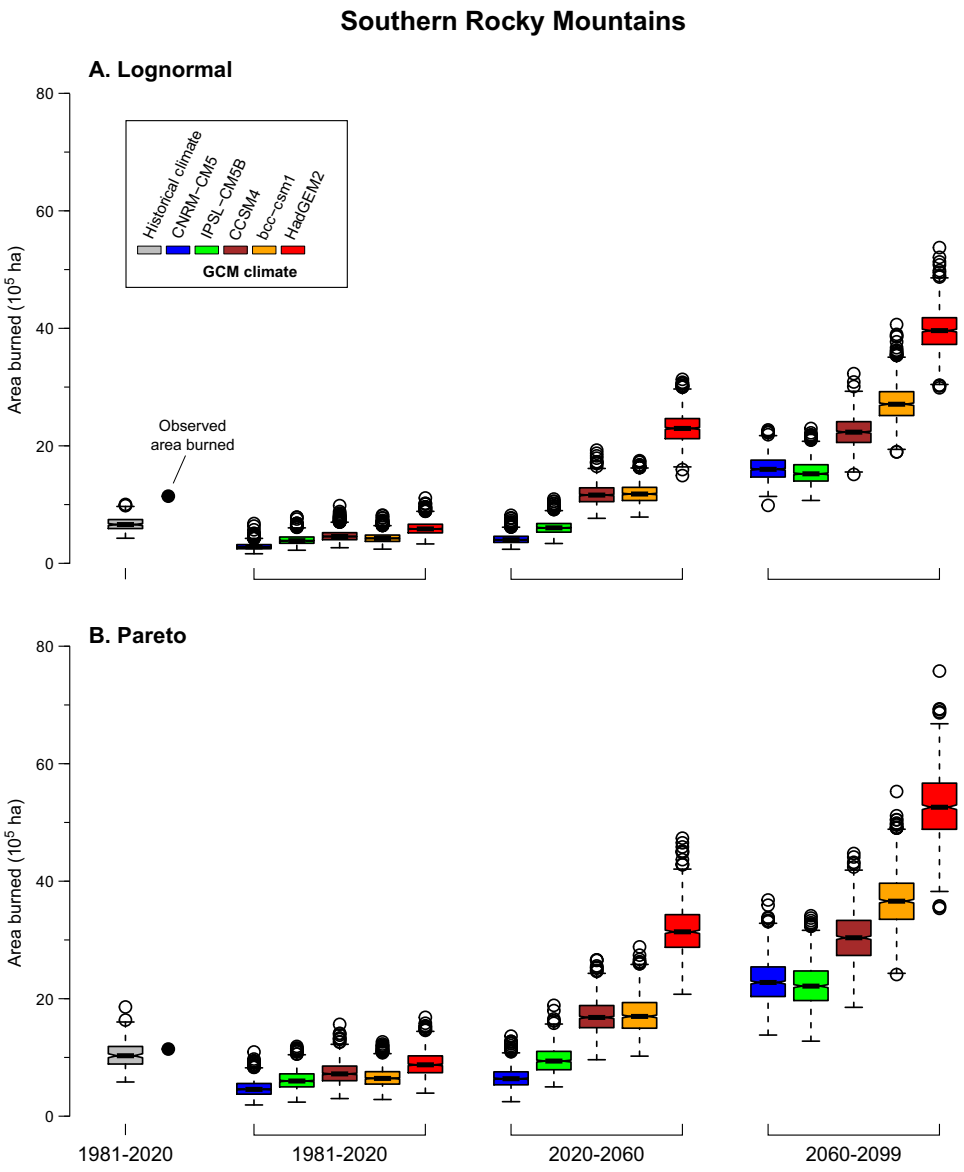

Fig. 6. Box plots of total simulated area burned in the Southern Rocky Mountains for three 40-year periods. Simulated fire sizes were drawn from lognormal (A) and Pareto (B) distributions that were fitted to observed fire-size data from 1980 – 2020. Gray box plots show simulations with historical climate, colored box plots used GCM climate. Black point shows observed area burned from 1981 – 2020.

States (Dillon et al., 2011; Parks and Abatzoglou, 2020), which indicates that typically moist settings, with higher fuel loads become flammable. Because we averaged aridity at the ecoregion scale, our ATs may identify fire seasons where a critical proportion of the landscape becomes flammable. Thus, during extensive fire years, fires readily spread among stands with distinct topographic settings and heterogeneous fuel moisture levels that in wetter years could restrict fire spread.

4.2. Influences on model performance

Model performance varied among ecoregions and with the choice of fire-size distribution type. Area burned models for ecoregions in the Rocky Mountains showed the highest skill and strongest correlations with observations (Table S1). In these ecoregions, interannual variation in fuel moisture exerts the strongest control on fire activity (Littell et al., 2018). Fine fuel availability can limit fire spread locally, e.g., in submontane *Pinus ponderosa* forests. However, at higher elevations in the Rocky Mountains, extensive subalpine forests have abundant, well-connected fuels that support high severity fire regimes and fire spread is limited primarily by fuel moisture (Sherriff and Veblen, 2008). In contrast, in the Mogollon Rim, where dry conditions and large fires are typical in most years, low model skill (Table S1) may relate to the importance of fine fuel limitations on fire activity, and also reflect the lack of distinction among fires with differing severities in our model. Woodlands and submontane forests with relatively open canopies and grassy understories are typical of the Mogollon Rim (Hurteau et al., 2014). Therefore, climatic factors that control interannual variation in fine fuel availability, especially antecedent moisture, may be needed in combination with current-year aridity to more effectively predict variations in area burned in ecoregions like the Mogollon Rim (Swetnam and Betancourt, 1990).

Extreme fire years affected the position of ATs and model skill in some ecoregions. For example, leaving out 2020 from the Sierra Nevada and Cascades ranges resulted in non-significant correlations between simulated and observed area burned over the 41-year calibration period, and large reductions in model skill. Thus, our leave-one-year-out models did not capture area burned in years when area burned vastly exceeded all previous observations. Similar situations may develop in other

ecoregions where extreme fire years that greatly exceeded previously observed area burned did not occur during the calibration period. For example, in the highly productive forests of the Northern Cascades and Oregon Coastal Range, average area burned is lower than other ecoregions, which may affect model fit and performance. Extensive burning in these ecoregions is highly episodic, and smaller fires exhibit weak climatic control (Colombaroli and Gavin, 2010). Therefore, the inclusion of more years, especially with extreme area burned may be necessary to precisely define ATs that identify extensive fire years. In contrast, multiple extreme fire years that can help characterize fire activity under extremely dry conditions occurred during the calibration period in the Southern Rocky Mountains (Fig. 2). Ultimately, while extreme fire years may shift ATs, inclusion of such years may be critical to identifying fire-season analogues for a warmer and drier future.

The value of accurately depicting annual versus decadal scale variations is an important consideration when selecting statistical distributions for area burned models. Pareto distributions better captured rare extreme events that dominate area burned on decadal scales in the western United States. Lognormal distributions more effectively reproduced interannual variability, as demonstrated by higher model skill, but are more likely to miss extreme fire events that can dominate ecological processes for decades. This difference results from the higher probability of rare, extreme events (i.e., very large fires) with Pareto distributions, and the resulting wider range of simulated area burned in our simulation replicates (Holmes et al., 2008). The statistical distribution that best characterizes fire-size distributions may also change through time (Li and Banerjee, 2021). For example, Pareto distributions may better approximate fire sizes as the proportion of area burned incurred during extreme fire events increases in a warming climate, as is likely in ecosystems with flammability-limited fire regimes (Williams et al., 2019).

Changes in fuel availability and fire suppression policies and/or efficacy may affect the long-term stability of ATs by changing relationships between fire spread and climate (Higuera et al., 2015; Taylor et al., 2016). In several ecoregions with increasing trends in area burned during the calibration period (e.g., Sierra Nevada Range, Mogollon Rim, Southern Rocky Mountains), we overestimated area burned during the 1980s and/or 1990s but underestimated during the 2020s (Figs. 3 and S3). Observed increases in area burned relate in part to increasing temperatures and fuel aridity between these intervals (Abatzoglou and Williams, 2016). However, model performance may have also been affected by the changing success of fire suppression in these decades. That is, fire suppression limited area burned during the relatively moist 1980s but was less successful during the historically dry 2010s as the number of days and amount of area experiencing extreme fire danger increased (Abatzoglou et al., 2021b). Changes in fire suppression policies may also have had a modest effect on our results. After 2009, fire managers were granted greater flexibility to allow some fires to burn, especially in wilderness areas, which may have also contributed to our underestimate of area burned in the Rocky Mountains and Mogollon Rim in the 2010s (Young et al., 2020).

4.3. Implications from the Southern Rocky Mountains for projecting area burned in a warming climate

Our threshold approach does not extrapolate beyond observed climate-fire relationships to project area burned in a warming climate. Although we calibrated our model with recent fire years, we identified ATs that distinguish significant differences in annual area burned and draw fire sizes from distributions defined by these thresholds. Therefore, median area burned in our simulations approaches the maximum of past observed annual area burned (Figs. 4 and 5). Nonetheless, because fire sizes are generated randomly, maximum simulated area burned can exceed maximum observed area burned, especially as the number of large fires increases with FSCWD (Figs. 2 and 3). Furthermore, decadal area burned can also exceed observations as the frequency of extensive fire years (i.e., FSCWD > AT2) increases.

A key challenge for projecting area burned in a warmer and drier future is that fire-climate relationships change through time; they are non-stationary (Gavin et al., 2007; McKenzie and Littell, 2017). For example, climate was a stronger predictor of area burned during recent decades than during the mid-20th century for many ecoregions in the western United States (Higuera et al., 2015; Littell et al., 2009). Thus, area burned models developed for one period can over or underpredict fire when applied to novel climate conditions. Vegetation change is an important driver of non-stationarity. Changing climate and disturbance regimes can alter fuel accumulation, decomposition, and structure, which affects fire spread and ultimately area burned (Batllori et al., 2013; Matthews et al., 2012; Parks et al., 2018). Consequently, as with other models, our simulations become less reliable as the frequency of extensive fire years increases and climate departs from the historical range of variation under which our models were trained (Littell et al., 2018; Westerling et al., 2011), especially if interactions between wildfires and drought stress alter forest regeneration (Davis et al., 2019). Littell et al. (2018) concluded that simulated fire rotations for an ecoregion that are shorter than the calibration period of a statistical area burned model violate the assumption that future vegetation will resemble historical vegetation and therefore support a similar fire-climate relationship. Similar inferences can be made from our approach. Once most years pass the threshold for extensive area burned, it is unlikely that vegetation will support the fire-climate relationships observed during the calibration period. For the Southern Rocky Mountains, the timing of such a shift varies among GCMs from after 2038 under the extreme HadGEM2, but not until the 2090s with the wetter CNRM-CM5 and IPSL-CM5B GCMs (Figs. 4a, 5a). Thus, although we project major increases in area burned under all GCMs (Fig. 6), the timing of departure from observed fire-climate relationships will likely depend on changes in future precipitation regimes, which have higher uncertainty than temperature projections (Woldemeskel et al., 2016).

Statistical area burned models can attenuate projected area burned in a warming climate to account for vegetation feedbacks to fire-climate relationships (Abatzoglou et al., 2021a; Turco et al., 2018). However, calibrating vegetation feedbacks in area burned simulations is nontrivial because the specific impacts of vegetation change on fire regimes vary among forest types and ecoregions (Gavin et al., 2007; Tepley et al., 2018). In projections of area burned for the western United States, Abatzoglou et al. (2021a) limited area burned in a warming climate following the assumptions that fire-fuel feedbacks diminish the forest area capable of carrying subsequent fires and that fuel limitations can diminish through time. These authors concluded that fuel availability will impart only a modest limitation on forest area burned through the mid-century relative to climate-driven increases in flammability. Climate change and fire activity can also have positive feedbacks on area burned. Climate and fire-driven shifts that reduce tree density or trigger forest to shrubland or grassland conversion can increase fine fuel availability and promote short-interval burning, even if fire intensity is reduced (Coop et al., 2020; Tepley et al., 2018). Therefore, assumptions that fire activity and/or warming will limit future area burned are not always justified and in projecting area burned, the range of GCM uncertainty may be greater than uncertainty in changes to fire-climate feedbacks (Turco et al., 2018). One way to address the shortcomings of purely statistical modeling approaches is to couple statistical models with landscape simulation models. In this approach, the statistical model would provide regional targets to the landscape simulation model for area burned, or fire-size distributions that change with future weather and climate conditions. However, the landscape simulation model would determine the actual area burned, accounting for spatial variability in biomass and how that variability was altered by past fires and other disturbances. We have used this approach, coupling our aridity threshold fire model with the LANDIS-II forest landscape model, which tracks fire spread across landscapes in addition to species establishment, growth rates, and biomass levels (Henne et al., 2021). Future

efforts could also dynamically adjust aridity thresholds to depict climatically driven changes in fuel. For example, Pausas and Paula (2012) found a positive linear relationship between aridity thresholds and productivity among 13 regions in Spain that could be applied to dynamically adjust aridity thresholds in a changing climate.

5. Conclusions

Our aridity threshold fire model relates the annual number and size of wildfires to fire-season aridity to simulate climate-driven changes in annual area burned at the ecoregion scale. By applying thresholds in area burned, our model projects abrupt changes in annual area burned that result as the frequency of extreme fire seasons increases, with major increases after 2020 for most GCMs, and all GCMs after 2060. Because our model requires limited inputs it can be readily updated to incorporate recent observations and the knowledge gained from future extreme fire years. Such adaptability may be critical in the western United States and other regions where climatic conditions and fire regimes are rapidly diverging from past observations (Higuera and Abatzoglou, 2021), but also allows application of our model at broader scales. Our statistical model is robust enough to be used on its own to project the timing of major changes in annual area burned, but also applicable to models that directly simulate feedbacks among climate, vegetation, land use, and fire. For example, forest landscape models (Henne et al., 2021) or state and transition models (Sleeter et al., 2015; Marchal et al., 2020) that require ignition counts and fire size distributions to simulate wildfire, which our AT model produces. Similarly, we provide a low complexity alternative for fire-enabled DGVMs (Hantsen et al. 2016) that directly calibrates thresholds in fire-season moisture and makes few assumptions about fire spread. Development of empirical relationships between climatic thresholds for extensive fire years over gradients in productivity and aridity could further the applicability of our approach to global fire models (Pausas and Paula, 2012).

CRediT author statement

For an aridity threshold model of fire sizes and annual area burned in extensively forested ecoregions of the Western USA, by Paul D. Henne and Todd J. Hawbaker.

Data availability

Model outputs are openly available in Henne and Hawbaker (2023), https://doi.org/10.5066/P9ERJ5Z4.

CRediT authorship contribution statement

Paul D. Henne: Conceptualization, Methodology, Investigation, Writing – original draft. **Todd J. Hawbaker:** Conceptualization, Methodology, Writing – review & editing, Funding acquisition.

Declaration of Competing Interest

The authors declare that they have no known competing financial interests or personal relationships that could have appeared to influence the work reported in this paper.

Data availability

Model outputs are openly available in Henne and Hawbaker (2023), https://doi.org/10.5066/P9ERJ5Z4

Acknowledgements

This research was funded by the U.S. Geological Survey (USGS) Climate Research and Development and Biologic Carbon Sequestration Assessment (LandCarbon) programs and by the North Central Climate Adaptation Science Center, which is managed by the USGS National Climate Adaptation Science Center. We thank Hong S. He and three anonymous reviews whose comments helped improve the manuscript. Jeremy Havens improved the figures. Any use of trade, firm, or product names is for descriptive purposes only and does not imply endorsement by the U.S. Government.

Supplementary materials

Supplementary material associated with this article can be found, in the online version, at doi:10.1016/j.ecolmodel.2023.110277.

References

Abatzoglou, J.T., 2013. Development of gridded surface meteorological data for ecological applications and modelling. Int. J. Climatol. 33, 121–131. https://doi.org/10.1002/joc.3413.

Abatzoglou, J.T., Battisti, D.S., Williams, A.P., Hansen, W.D., Harvey, B.J., Kolden, C.A., 2021a. Projected increases in western US forest fire despite growing fuel constraints. Commun. Earth Environ. 2, 227. https://doi.org/10.1038/s43247-021-00299-0.

Abatzoglou, J.T., Brown, T.J., 2012. A comparison of statistical downscaling methods suited for wildfire applications. Int. J. Climatol. 32, 772–780. https://doi.org/10.1002/joc.2312.

Abatzoglou, J.T., Juang, C.S., Williams, A.P., Kolden, C.A., Westerling, A.L., 2021b. Increasing synchronous fire danger in forests of the Western United States. Geophys. Res. Lett. 48 https://doi.org/10.1029/2020GL091377 e2020GL091377.

Abatzoglou, J.T., Kolden, C.A., 2013. Relationships between climate and macroscale area burned in the western United States. Int. J. Wildl. Fire 22, 1003–1020. https://doi.org/10.1071/WF13019.

Abatzoglou, J.T., Williams, A.P., 2016. Impact of anthropogenic climate change on wildfire across western US forests. Proc. Natl. Acad. Sci 113, 11770–11775. https://doi.org/10.1073/pnas.1607171113.

Batllori, E., Parisien, M.A., Krawchuk, M.A., Moritz, M.A., 2013. Climate change-induced shifts in fire for Mediterranean ecosystems. Glob. Ecol. Biogeogr. 22, 1118–1129. https://doi.org/10.1111/geb.12065.

Bond, W.J., Woodward, F.I., Midgley, G.F., 2005. The global distribution of ecosystems in a world without fire. New Phytol 165, 525–538. https://doi.org/10.1111/j.1469-8137.2004.01252.x.

Bowman, D.M.J.S., Balch, J.K., Artaxo, P., Bond, W.J., Carlson, J.M., Cochrane, M.A., D'Antonio, C.M., DeFries, R.S., Doyle, J.C., Harrison, S.P., Johnston, F.H., Keeley, J. E., Krawchuk, M.A., Kull, C.A., Marston, J.B., Moritz, M.A., Prentice, I.C., Roos, C.I., Scott, A.C., Swetnam, T.W., van der Werf, G.R., Pyne, S.J., 2009. Fire in the earth system. Science (80-.). 324, 481–484. https://doi.org/10.1126/science.1163886.

Bowman, D.M.J.S., Williamson, G.J., Abatzoglou, J.T., Kolden, C.A., Cochrane, M.A., Smith, A.M.S., 2017. Human exposure and sensitivity to globally extreme wildfire events. Nat. Ecol. Evol. 1, 58. https://doi.org/10.1038/s41559-016-0058.

Calder, W.J., Parker, D., Stopka, C.J., Jiménez-Moreno, G., Shuman, B.N., 2015. Medieval warming initiated exceptionally large wildfire outbreaks in the Rocky Mountains. Proc. Natl. Acad. Sci 112, 13261–13266. https://doi.org/10.1073/pnas.1500796112.

Collins, L., Bradstock, R.A., Clarke, H., Clarke, M.F., Nolan, R.H., Penman, T.D., 2021. The 2019/2020 mega-fires exposed Australian ecosystems to an unprecedented extent of high-severity fire. Environ. Res. Lett. 16, 044029 https://doi.org/10.1088/1748-9326/abeb9e.

Colombaroli, D., Gavin, D.G., 2010. Highly episodic fire and erosion regime over the past 2,000 y in the Siskiyou Mountains, Oregon. Proc. Natl. Acad. Sci. 107, 18909–18914. https://doi.org/10.1073/pnas.1007692107.

Coop, J.D., Parks, S.A., Stevens-Rumann, C.S., Crausbay, S.D., Higuera, P.E., Hurteau, M. D., Tepley, A., Whitman, E., Assal, T., Collins, B.M., Davis, K.T., Dobrowski, S., Falk, D.A., Fornwalt, P.J., Fulé, P.Z., Harvey, B.J., Kane, V.R., Littlefield, C.E., Margolis, E.Q., North, M., Parisien, M.A., Prichard, S., Rodman, K.C., 2020. Wildfire-driven forest conversion in Western North American landscapes. Bioscience 70, 659–673. https://doi.org/10.1093/biosci/biaa061.

Davis, K.T., Dobrowski, S.Z., Higuera, P.E., Holden, Z.A., Veblen, T.T., Rother, M.T., Parks, S.A., Sala, A., Maneta, M.P., 2019. Wildfires and climate change push low-elevation forests across a critical climate threshold for tree regeneration. Proc. Natl. Acad. Sci. 116, 6193–6198. https://doi.org/10.1073/pnas.1815107116.

Delignette-Muller, M.L., Dutang, C., 2015. fitdistrplus: an r package for fitting distributions. J. Stat. Softw. 64, 1–34. https://doi.org/10.18637/jss.v064.i04.

Dillon, G.K., Holden, Z.A., Morgan, P., Crimmins, M.A., Heyerdahl, E.K., Luce, C.H., 2011. Both topography and climate affected forest and woodland burn severity in two regions of the western US, 1984 to 2006 Ecosphere 2, 1–33. https://doi.org/10.1890/ES11-00271.1.

Finney, M.A., Grenfell, I.C., McHugh, C.W., Seli, R.C., Trethewey, D., Stratton, R.D., Brittain, S., 2011. A method for ensemble wildland fire simulation. Environ. Model. Assess. 16, 153–167. https://doi.org/10.1007/s10666-010-9241-3.

Gavin, D.G., Hallett, D.J., Hu, F.S., Lertzman, K.P., Prichard, S.J., Brown, K.J., Lynch, J. A., Bartlein, P.J., Peterson, D.L., 2007. Forest fire and climate change in western North America: insights from sediment charcoal records. Front. Ecol. Environ. 5, 499–506. https://doi.org/10.1890/060161.

Hantson, S., Arneth, A., Harrison, S.P., Kelley, D.I., Colin Prentice, I., Rabin, S.S., Archibald, S., Mouillot, F., Arnold, S.R., Artaxo, P., Bachelet, D., Ciais, P., Forrest, M., Friedlingstein, P., Hickler, T., Kaplan, J.O., Kloster, S., Knorr, W., Lasslop, G., Li, F., Mangeon, S., Melton, J.R., Meyn, A., Sitch, S., Spessa, A., van der Werf, G.R., Voulgarakis, A., Yue, C., 2016. The status and challenge of global fire modelling. Biogeosciences 13, 3359–3375. https://doi.org/10.5194/bg-13-3359-2016.

He, H.S., Mladenoff, D.J., 1999. Spatially explicit and stochastic simulation of forest-landscape fire disturbance and succession. Ecology 80, 81–99. https://doi.org/10.1890/0012-9658(1999)080[0081:SEASSO]2.0.CO;2.

Henne, P.D., Hawbaker, T.J., Scheller, R.M., Zhao, F., He, H.S., Xu, W., Zhu, Z., 2021. Increased burning in a warming climate reduces carbon uptake in the Greater Yellowstone Ecosystem despite productivity gains. J. Ecol. 109, 1148–1169. https://doi.org/10.1111/1365-2745.13559.

Higuera, P.E., Abatzoglou, J.T., 2021. Record-setting climate enabled the extraordinary 2020 fire season in the western United States. Glob. Chang. Biol. 27, 1–2. https://doi.org/10.1111/gcb.15388.

Higuera, P.E., Abatzoglou, J.T., Littell, J.S., Morgan, P., 2015. The changing strength and nature of fire-climate relationships in the Northern Rocky Mountains, U.S.A., 1902-2008. PLoS ONE 10, e0127563. https://doi.org/10.1371/journal.pone.0127563.

Higuera, P.E., Shuman, B.N., Wolf, K.D., 2021. Rocky Mountain subalpine forests now burning more than any time in recent millennia. Proc. Natl. Acad. Sci. 118, 1–5. https://doi.org/10.1073/pnas.2103135118.

Henne, P.D., and Hawbaker, T.J., 2023. Simulated annual area burned for eleven extensively forested ecoregions in the western United States for 1980 –2099. U.S. Geological Survey data release. 10.5066/P9ERJ5Z4.

Holmes, T.P., Huggett, R.J., Westerling, A.L., 2008. Statistical Analysis of Large Wildfires BT - The Economics of Forest Disturbances: Wildfires, Storms, and Invasive Species, in: Holmes, T.P., Prestemon, J.P., Abt, K.L. (Eds.), Springer Netherlands, Dordrecht, pp. 59–77. https://doi.org/10.1007/978-1-4020-4370-3_4.

Homer, C., Dewitz, J., Yang, L., Jin, S., Danielson, P., Xian, G., Coulston, J., Herold, N., Wickham, J., Megown, K., 2015. Completion of the 2011 National Land Cover Database for the Conterminous United States–representing a decade of land cover change information. Photogramm. Eng. Remote Sens. 81, 345–354.

Hothorn, T., Hornik, K., Zeileis, A., 2006. Unbiased recursive partitioning: a conditional inference framework. J. Comput. Graph. Stat. 15, 651–674. https://doi.org/10.1198/106186006X133933.

Hurteau, M.D., Bradford, J.B., Fulé, P.Z., Taylor, A.H., Martin, K.L., 2014. Climate change, fire management, and ecological services in the southwestern US. For. Ecol. Manage. 327, 280–289. https://doi.org/10.1016/j.foreco.2013.08.007.

Jain, P., Coogan, S.C.P., Subramanian, S.G., Crowley, M., Taylor, S., Flannigan, M.D., 2020. A review of machine learning applications in wildfire science and management. Environ. Rev. 28, 478–505. https://doi.org/10.1139/er-2020-0019.

Kane, V.R., Lutz, J.A., Alina Cansler, C., Povak, N.A., Churchill, D.J., Smith, D.F., Kane, J. T., North, M.P., 2015. Water balance and topography predict fire and forest structure patterns. For. Ecol. Manage. 338, 1–13. https://doi.org/10.1016/j.foreco.2014.10.038.

Li, F., Zeng, X.D., Levis, S., 2012. A process-based fire parameterization of intermediate complexity in a dynamic global vegetation model. Biogeosciences 9, 2761–2780. https://doi.org/10.5194/bg-9-2761-2012.

Li, S., Banerjee, T., 2021. Spatial and temporal pattern of wildfires in California from 2000 to 2019. Sci. Rep. 11, 1–17. https://doi.org/10.1038/s41598-021-88131-9.

Liang, S., Hurteau, M.D., Westerling, A.L., 2017. Response of Sierra Nevada forests to projected climate-wildfire interactions. Glob. Chang. Biol. 23 https://doi.org/10.1111/gcb.13544, 2016–2030.

Littell, J.S., McKenzie, D., Peterson, D.L., Westerling, A.L., 2009. Climate and wildfire area burned in western U.S. ecoprovinces, 1916–2003. Ecol. Appl. 19, 1003–1021. https://doi.org/10.1890/07-1183.1.

Littell, J.S., McKenzie, D., Wan, H.Y., Cushman, S.A., 2018. Climate change and future wildfire in the Western United States: an ecological approach to nonstationarity. Earth's Futur. https://doi.org/10.1029/2018EF000878.

Littell, J.S., Peterson, D.L., Riley, K.L., Liu, Y., Luce, C.H., 2016. A review of the relationships between drought and forest fire in the United States. Glob. Chang. Biol. 22, 2353–2369. https://doi.org/10.1111/gcb.13275.

Liu, Z., Wimberly, M.C., Lamsal, A., Sohl, T.L., Hawbaker, T.J., 2015. Climate change and wildfire risk in an expanding wildland–urban interface: a case study from the Colorado Front Range Corridor. Landsc. Ecol. 30, 1943–1957. https://doi.org/10.1007/s10980-015-0222-4.

Marchal, J., Cumming, S.G., McIntire, E.J.B., 2020. Turning down the heat: vegetation feedbacks limit fire regime responses to global warming. Ecosystems 23, 204–216. https://doi.org/10.1007/s10021-019-00398-2.

Matthews, S., Sullivan, A.L., Watson, P., Williams, R.J., 2012. Climate change, fuel and fire behaviour in a eucalypt forest. Glob. Chang. Biol. 18, 3212–3223. https://doi.org/10.1111/j.1365-2486.2012.02768.x.

Marlon, J.R., Bartlein, P.J., Gavin, D.G., Long, C.J., Anderson, R.S., Briles, C.E., Brown, K. J., Colombaroli, D., Hallett, D.J., Power, M.J., Scharf, E.A., Walsh, M.K., 2012. Long-term perspective on wildfires in the western USA. Proc. Natl. Acad. Sci 109, E535–E543. https://doi.org/10.1073/pnas.1112839109.

McCabe, G.J., Wolock, D.M., 2021. Water balance of the turn-of-the-century drought in the Southwestern United States. Environ. Res. Lett. 16, 044015 https://doi.org/10.1088/1748-9326/abbfc1.

McKenzie, D., Littell, J.S., 2017. Climate change and the eco-hydrology of fire: will area burned increase in a warming western USA. Ecol. Appl. 27, 26–36. https://doi.org/10.1002/eap.1420.

Parks, S.A., Abatzoglou, J.T., 2020. Warmer and drier fire seasons contribute to increases in area burned at high severity in Western US forests from 1985 to 2017. Geophys. Res. Lett. 47 https://doi.org/10.1029/2020GL089858 e2020GL089858.

Parks, S.A., Parisien, M.A., Miller, C., Holsinger, L.M., Baggett, L.S., 2018. Fine-scale spatial climate variation and drought mediate the likelihood of reburning. Ecol. Appl. 27, 573–586. https://doi.org/10.1002/eap.1671.

Pausas, J.G., Paula, S., 2012. Fuel shapes the fire-climate relationship: evidence from Mediterranean ecosystems. Glob. Ecol. Biogeogr. 21, 1074–1082. https://doi.org/10.1111/j.1466-8238.2012.00769.x.

Ponomarev, E., Yakimov, N., Ponomareva, T., Yakubailik, O., Conard, S.G., 2021. Current trend of carbon emissions from wildfires in Siberia. Atmosphere (Basel) 12, 1–15. https://doi.org/10.3390/atmos12050559.

R. Core Team, 2022. R: A Language and Environment For Statistical Computing. R Foundation for Statistical Computing, Vienna, Austria. https://www.R-project.org/.

Rollins, M.G., Morgan, P., Swetnam, T.W., 2002. Landscape-scale controls over 20th century fire occurrence in two large Rocky Mountain (USA) wilderness areas. Landsc. Ecol. 17, 539–557. https://doi.org/10.1023/A:1021584519109.

Scheller, R.M., Lucash, M.S., Kretchun, A., Henne, P.D., Haga, C., Hotta, W., 2021. LANDIS-II NECN succession v6. 7 Extension user guide.

Sherriff, R.L., Veblen, T.T., 2008. Variability in fireclimate relationships in ponderosa pine forests in the Colorado Front Range. Int. J. Wildl. Fire 17, 50–59.

Short, K.C., 2021. Spatial wildfire occurrence data for the United States, 1992-2018 [FPA_FOD_20210617], 5th ed. Forest Service Research Data Archive, Fort Collins, CO. https://doi.org/10.2737/RDS-2013-0009.5.

Sleeter, B.M., Liu, J., Daniel, C., Frid, L., Zhu, Z., 2015. An integrated approach to modeling changes in land use, land cover, and disturbance and their impact on ecosystem carbon dynamics: a case study in the Sierra Nevada Mountains of California. AIMS Env. Sci 2, 577–606. https://doi.org/10.3934/environsci.2015.3.577.

Stephenson, N.L., 1998. Actual evapotranspiration and deficit: biologically meaningful correlates of vegetation distribution across spatial scales. J. Biogeogr. 25, 855–870. https://doi.org/10.1046/j.1365-2699.1998.00233.x.

Swetnam, T.W., Betancourt, J.L., 1990. Fire-southern oscillation relations in the Southwestern United States. Science (80-.) 249, 1017–1020. https://doi.org/10.1126/science.249.4972.1017.

Taylor, A.H., Trouet, V., Skinner, C.N., Stephens, S., 2016. Socioecological transitions trigger fire regime shifts and modulate fire–climate interactions in the Sierra Nevada, USA, 1600–2015 CE. Proc. Natl. Acad. Sci. 113, 13684–13689. https://doi.org/10.1073/pnas.1609775113.

Tepley, A.J., Thomann, E., Veblen, T.T., Perry, G.L.W., Holz, A., Paritsis, J., Kitzberger, T., Anderson-Teixeira, K.J., 2018. Influences of fire–vegetation feedbacks and post-fire recovery rates on forest landscape vulnerability to altered fire regimes. J. Ecol. 106, 1925–1940. https://doi.org/10.1111/1365-2745.12950.

Thonicke, K., Venevsky, S., Sitch, S., Cramer, W., 2001. The role of fire disturbance for global vegetation dynamics: coupling fire into a dynamic global vegetation model. Glob. Ecol. Biogeogr. https://doi.org/10.1046/j.1466-822X.2001.00175.x.

Turco, M., Rosa-Cánovas, J.J., Bedia, J., Jerez, S., Montávez, J.P., Llasat, M.C., Provenzale, A., 2018. Exacerbated fires in Mediterranean Europe due to anthropogenic warming projected with non-stationary climate-fire models. Nat. Commun. 9, 1–9. https://doi.org/10.1038/s41467-018-06358-z.

Turner, M.G., 2010. Disturbance and landscape dynamics in a changing world 1. Ecology 91, 2833–2849. https://doi.org/10.1890/10-0097.1.

Westerling, A.L., Gershunov, A., Brown, T.J., Cayan, D.R., Dettinger, M.D., 2003. Climate and wildfire in the Western United States. Bull. Am. Meteorol. Soc. 84, 595–604. https://doi.org/10.1175/BAMS-84-5-595.

Westerling, A.L., Hidalgo, H.G., Cayan, D.R., Swetnam, T.W., 2006. Warming and earlier spring increase Western U.S. forest wildfire activity. Science (80-.) 313, 940–943. https://doi.org/10.1126/science.1128834.

Westerling, A.L., Turner, M.G., Smithwick, E.A.H., Romme, W.H., Ryan, M.G., 2011. Continued warming could transform Greater Yellowstone fire regimes by mid-21st century. Proc. Natl. Acad. Sci. 108, 13165–13170. https://doi.org/10.1073/pnas.1110199108.

Williams, A.P., Abatzoglou, J.T., Gershunov, A., Guzman-Morales, J., Bishop, D.A., Balch, J.K., Lettenmaier, D.P., 2019. Observed impacts of anthropogenic climate change on wildfire in California. Earth's Futur 7, 892–910. https://doi.org/10.1029/2019EF001210.

Williams, A.P., Cook, E.R., Smerdon, J.E., Cook, B.I., Abatzoglou, J.T., Bolles, K., Baek, S. H., Badger, A.M., Livneh, B., 2020. Large contribution from anthropogenic warming to an emerging North American megadrought. Science 368, 314–318. https://doi.org/10.1126/science.aaz9600.

Williams, A.P., Seager, R., Macalady, A.K., Berkelhammer, M., Crimmins, M.A., Swetnam, T.W., Trugman, A.T., Buenning, N., Noone, D., McDowell, N.G., Hryniw, N., Mora, C.I., Rahn, T., 2015. Correlations between components of the water balance and burned area reveal new insights for predicting forest fire area in the southwest United States. Int. J. Wildl. Fire 24, 14. https://doi.org/10.1071/WF14023.

Woldemeskel, F.M., Sharma, A., Sivakumar, B., Mehrotra, R., 2016. Quantification of precipitation and temperature uncertainties simulated by CMIP3 and CMIP5 models. J. Geophys. Res. Atmos. 121, 3–17. https://doi.org/10.1002/2015JD023719.

Xi, D.D.Z., Taylor, S.W., Woolford, D.G., Dean, C.B., 2019. Statistical models of key components of wildfire risk. Annu. Rev. Stat. Its Appl. 6, 197–222. https://doi.org/10.1146/annurev-statistics-031017-100450.

Young, A.M., Higuera, P.E., Duffy, P.A., Hu, F.S., 2017. Climatic thresholds shape northern high-latitude fire regimes and imply vulnerability to future climate change. Ecography (Cop.) 40, 606–617. https://doi.org/10.1111/ecog.02205.

Young, J.D., Evans, A.M., Iniguez, J.M., Thode, A., Meyer, M.D., Hedwall, S.J., McCaffrey, S., Shin, P., Huang, C.H., 2020. Effects of policy change on wildland fire management strategies: evidence for a paradigm shift in the western US? Int. J. Wildl. Fire 29, 857–877. https://doi.org/10.1071/WF19189.